Application Note

November 2023

Rapid Development of an Amorphous Solid Dispersion (ASD) – Nifedipine (NIF)

Nico Setiawan, Ph.D., Cameron Bergman,
Triclinic Labs, Inc.

Amorphous solid dispersions (ASD) have long been used to increase the solubility and bioavailability of poorly-soluble compounds. A considerable amount of research has been carried out and has generated useful techniques in the area of ASD development. Surprisingly, the number of examples with successful application of the available techniques has been meager. Herein, a case study with nifedipine is presented where ASD candidates were rapidly determined within 2-3 weeks by utilizing a compilation of these techniques.

Keywords: Amorphous Solid Dispersion (ASD), Spray Drying, Crystallization, Solubility, Stability, Dissolution

Triclinic Labs
Chemical Development and Analysis Expertise

2660 Schuyler Ave, Suite A, Lafayette, IN 47905 USA
+1.765.588.6200 *www.tricliniclabs.com*

Introduction

Advancements in the drug discovery field have brough forth molecules with strong affinity for the intended biological targets [1]. While on one hand more efficacious drug molecules are generated, this process has created an immense solubility challenge for formulators as more hydrophobic drugs are also produced. It is estimated that between 70-90% of the current new chemical entities are poorly soluble [2]. Solubility of a compound is governed by the following: the energy required to break solute-solute and solvent-solvent interaction along with the energy gain from solute-solvent interaction. Typically, approaches for decreasing the solute-solute interaction, such as metastable polymorphs [3], cocrystals [4], and amorphous solid dispersions (ASD) [5], or increasing the solute-solvent interaction, such as complexation [6] and lipid-based delivery [7], are utilized in the pharmaceutical arena for solubility enhancement. In an ASD, the drug is “dissolved” in a polymeric matrix (or at least no long-range order solute-solute interaction exists in ASD though short-range interaction may exist), thus higher solubility is observed.

While there are many currently-marketed drug products formulated as ASDs [8], not every molecule may be amenable for ASD development. Ample techniques, from determining the glass stability [9] and amorphous solubility advantage [10-12] of the drug to screening polymers that best stabilize the amorphous drug [13-15], have been reported in the literature. In theory these can be used to rationally guide the development of ASD. Surprisingly, the collective application of these techniques on the ASD development of poorly-soluble molecules has not been widely exemplified. With the growing supply of poorly-soluble compounds and demand of rapid formulation development of these compounds, there is a need to compile the aforementioned techniques for rapid development of ASDs. Herein, these techniques are compiled to develop a rational screening process for the ASD development of a poorly-soluble compound, Nifedipine (NIF), with several commonly-used polymers: Eudragit L100, polyvinylpyrrolidone (PVP), polyvinylpyrrolidone vinyl acetate (PVPVA), hydroxypropyl methyl cellulose (HPMC), hydroxypropyl methyl cellulose phthalate (HPMCP), hydroxypropyl methyl cellulose acetate succinate (HPMCAS), hydroxypropyl cellulose (HPC), and polyacrylic acid (PAA). The chemical structures of materials used in this study are shown in Figure 1.

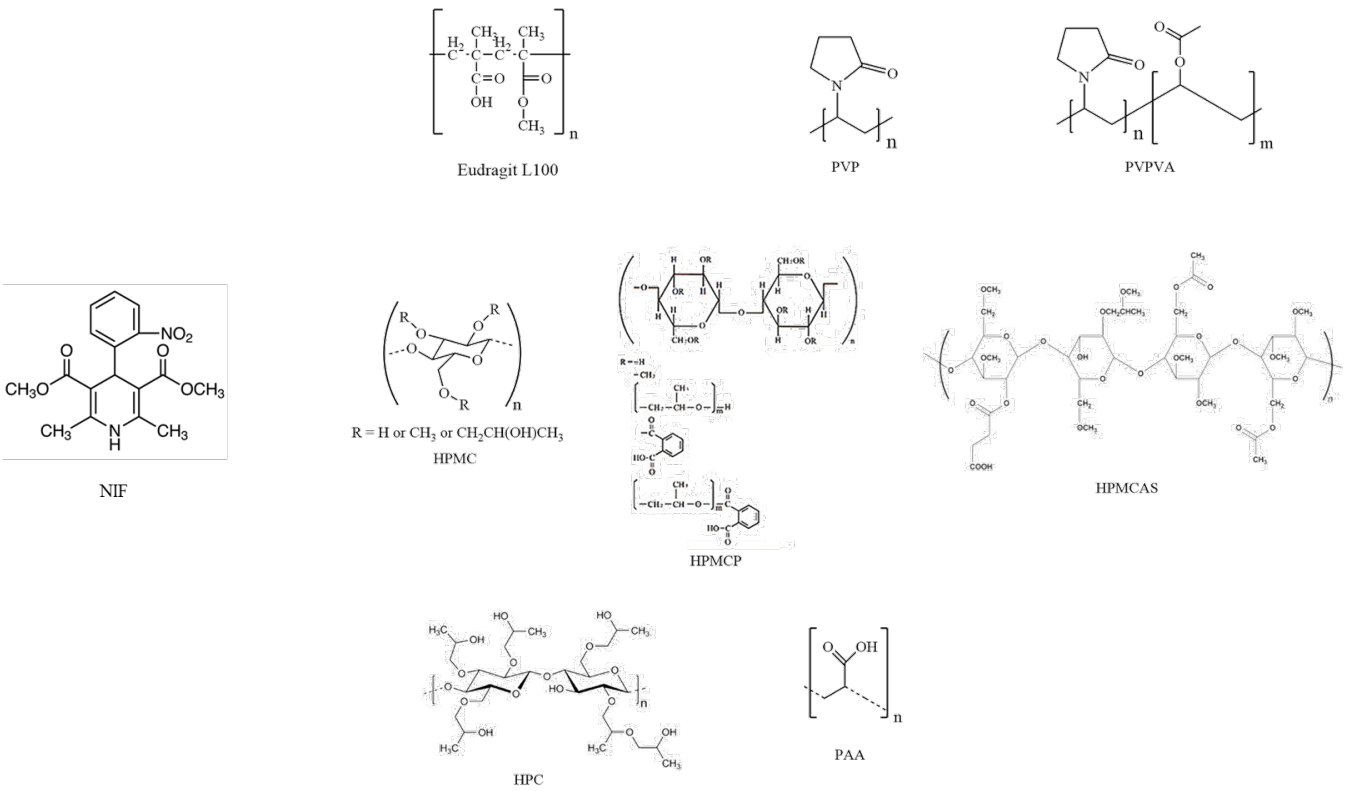

Figure 1. Chemical structures of NIF and polymers tested in this study: Eudragit L100, PVP, PVPVA, HPMC, HPMCP, HPMCAS, HPC, and PAA.

Materials and Methods

NIF was obtained from Alfa Aesar (Haverhill, MA). Polymers evaluated in this study were graciously supplied by the following manufacturers: Eudragit® L100 from Evonik (Essen, Germany), PVP K29/32 from Ashland (Wilmington, DE), HPMC K100 LV from Ashland (Wilmington, DE), HPMCP from Shin Etsu (Akron, OH), HPMCAS MG from Shin Etsu (Akron, OH), PVPVA from Ashland (Wilmington, DE), HPC LF (Klucel™) from Ashland (Wilmington, DE), and PAA Apinovex™ from Lubrizol (Wickliffe, OH).

Powder X-ray diffraction (PXRD) analyses were conducted on a Rigaku SmartLab X-ray diffractometer configured in Bragg–Brentano reflection geometry equipped with a beam stop and knife edge to reduce incident beam and air scatter. Data collection parameters are shown in Table 1.

Table 1. PXRD Data Collection Parameters

Parameter	Value
Geometry	Bragg-Brentano
Tube Anode	Cu Kα
Tube Type	Long Fine Focus
Tube Voltage (kV)	40
Tube Current (mA)	44
Detector	HyPix-3000
Monochromatization	Kβ Filter
Incident Slit (°)	1/3

Parameter	Value
Receiving Slit 1 (mm)	18
Receiving Slit 2 (mm)	20.1
Start Angle 2θ (°)	2
End Angle 2θ (°)	40
Step Size (°)	0.02
Scan Speed (°/min)	6
Spinning (rpm)	11
Sample Holder	Low background holder

Differential scanning calorimetry (DSC) analyses were carried out using a TA Instrument Q2000 Discovery Series instrument. The DSC cell was kept under a nitrogen purge of ~50 mL/min during the analysis. The sample was placed in a crimped Tzero aluminum pan and non-hermetically sealed and was equilibrated at 25°C. For a standard DSC analysis, the sample was heated at a rate of either 1 or 10 °C/min from ambient to 190 °C (past the melting point of NIF). For modulated DSC (mDSC), the sample was heated at 4 °C/min from ambient to 190 °C with a modulation of ±0.85 °C every 30 sec. For cyclic modulated DSC (mDSC), the following parameters were used: first heating at 10 °C/min from ambient to 190 °C and held for 3 min, cooling at -50 °C/min to 0 °C and held for 3 min, and a second heating at 4 °C/min to 190 °C with a modulation of ±0.85 °C every 30 sec.

Crystalline solubility was determined using a shake flask method. Excess NIF was added to a vial containing pH 6.8 phosphate buffer. The vial was agitated at 60 rpm in an incubator at 37 °C. After 24 hours, the sample was filtered using a 0.45 µm nylon syringe filter with the first 2 mL discarded and the remaining kept for analysis. The filtrate was analyzed by UV spectroscopy. Crystalline solubility measurement was performed in triplicate.

Amorphous solubility was determined using a solvent-shift method whereby small aliquots of a highly-concentrated solution of NIF in acetone were added to 20 mL of pH 6.8 phosphate buffer contained in a round bottom flask at 37 °C. Turbidity was monitored as a function of NIF concentration in the aqueous media via a turbidity probe (HEL CrystalEYES). Amorphous solubility was determined as the onset in increased turbidity was observed.

NIF spray dried dispersions (SDD) were generated by creating a 30-40 mg/mL solution of the listed ratio of NIF/polymer in methanol followed by spray drying via a ProCepT R&D spray dryer with 0.4 m^3/min inlet gas flow rate, 75 °C inlet gas temperature, 100 rpm solution pump speed, 0.3 bar nozzle gas pressure, and 2 bar cyclone gas pressure.

Dissolution studies were performed by adding 4 mL of pH 6.8 phosphate buffer into a vial containing pre-weighed NIF (either crystalline or spray dried dispersion (SDD)). Vials were placed in an incubator at 37 °C and agitated at 100 rpm. Aliquots of 0.5 mL were taken at specified time points and filtered with a pre-saturated 0.45 µm nylon syringe filter into new vials for analysis. Analysis was carried out using high-performance liquid chromatography (HPLC) via the following methodology: isocratic

mobile phase composition of 30:70 phosphate buffer pH 6.8/methanol, run time of 8 min, injection volume of 20 µL, detection wavelength at 236 nm, and a C18 Waters Symmetry column of 5.0 µm particle size and 4.6x250 mm dimension.

Polarized light microscopy (PLM) images were obtained using an Overstock binocular polarizing microscope. The slide was placed on the stage under the objective of 10x and 40x and illuminated with transmitted light. Multiple positions were analyzed with the microscope configured for cross-polarization with a red compensator.

Results and Discussion

Initial Characterization

Figure 2 shows the PXRD pattern of NIF starting material. The pattern is consistent with Form I of NIF [8]. In addition, the DSC data (top thermogram on the left image in Figure 3) shows a NIF melting point of 172 °C, confirming that the starting material was indeed Form I [16-17]. Crystalline NIF solubility was found to be 7.7 ± 2.2 µg/mL.

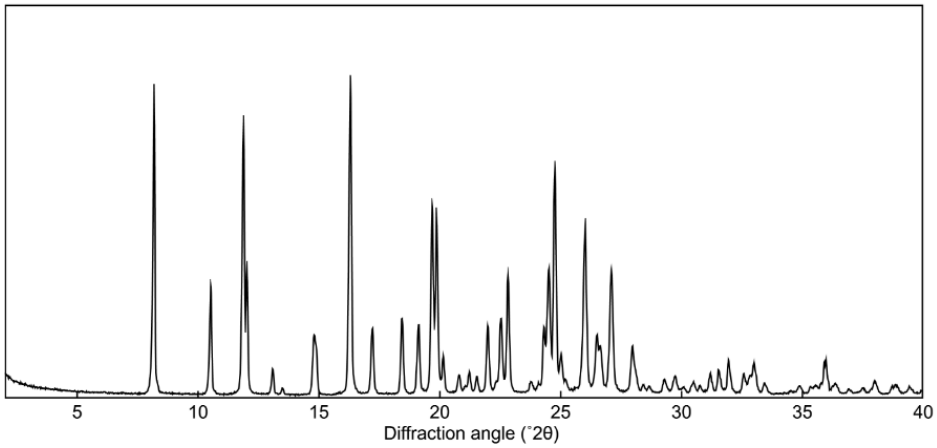

Figure 2. PXRD pattern of NIF starting material.

NIF ASD Feasibility Evaluation

Prior to developing the NIF ASD, two questions related to the properties of amorphous NIF should be answered: how stable is amorphous NIF and what is the amorphous solubility advantage? While it is true that the amorphous phase is metastable, the crystallization kinetics of each molecule could vary significantly. Thus, an estimation of crystallization kinetics is needed in rational ASD development. To address this, a cyclic mDSC analysis was conducted following a method published by Baird et al.

[9]. The method involves heating the compound past its melt followed by rapid cooling to a sufficiently low temperature and another heating cycle. The stability of the melt is then assessed by the point at which it re-crystallizes: Class I compound re-crystallizes during the cooling cycle, Class II during the second heating cycle, while Class III does not re-crystallize in the cyclic mDSC analysis. The result, as shown in Figure 3, shows that NIF glass forming ability (GFA) is class II where crystallization occurred on the second heating cycle. In addition, NIF glass transition temperature (T_g) was found to be 47 °C from the reversible heat flow data in the second heating cycle with modulation.

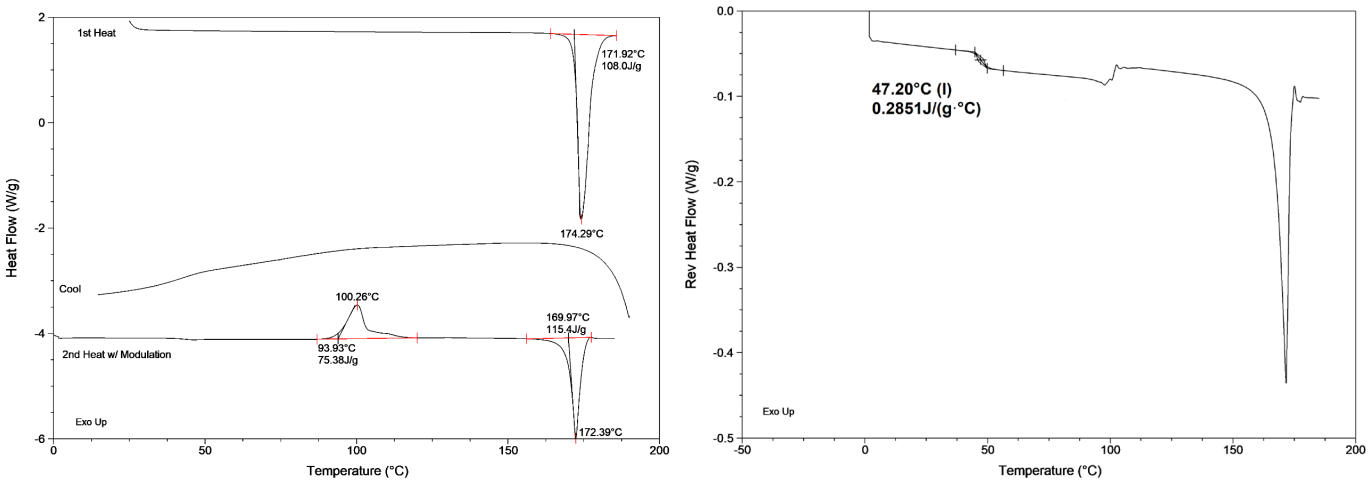

Figure 3. DSC data of NIF starting material. Left: cyclic mDSC thermogram where NIF was subjected to the first heating (top), rapid cooling (middle), and second heating with modulation (bottom). Right: reversible heat flow from the second heating cycle (bottom) of the left image.

Furthermore, an estimation of the amorphous solubility is required since this determination provides the extent of solubility (and potentially bioavailability) improvement over the crystalline phase. Literature suggests that the extent of amorphous solubility advantage could vary between 2 to 50-fold [12, 18] and is dependent on the test compound. However, a low solubility advantage should not necessarily discourage ASD development since a 2-fold advantage could mean doubled bioavailability for a solubility-limited absorption compound. The solubility advantage of amorphous NIF was determined experimentally following a method to find liquid-liquid phase separation (LLPS) as described by Ilevbare et al. [12]. The amorphous solubility value was found to be 304 µg/mL (Figure 4). This suggests that the amorphous solubility advantage is as high as approximately 40-fold (calculated by dividing the amorphous solubility by the crystalline solubility). However, it is worth noting that this value is likely overestimated due to the accumulation of NIF on the vial side walls above the liquid surface during the turbidity experiment.

Based on these data, a feasibility map for ASD development was proposed based on the drug GFA class and melt depression of drug-polymer physical mixture (see Polymer Selection below) as shown in Figure 5. Molecules that are most feasible for ASD development are those of GFA class II and III. GFA classification is determined via DSC where measurements are conducted under an inert (N_2) environment, thus the impact of other stresses, such as water (vapor during storage or aqueous

environment during dissolution), residual solvent (from solvent evaporation techniques), or mechanical stress in manufacturing, is not considered. Nevertheless, GFA classification provides a rapid assessment of drug crystallization behavior and, herein, is proposed as a screening method for ASD development feasibility. Indeed, Baird et al. [9] observed a correlation, though qualitative, between GFA and amorphous stability in the solid-state whereby faster crystallization was observed with lower GFA class molecules when these molecules were stressed at a temperature near (but below) their T_g and 0% RH. In general, GFA class I molecules are rapid crystallizers and very challenging to be developed as an ASD. Our experience with class I molecules (unpublished data), i.e., carbamazepine, tolbutamide, and tolfenamic acid, suggests that developing an ASD of these molecules will be very challenging unless a high melting point depression (≥ 10 °C) of the drug-polymer physical mixture is observed. No crystallization was observed in the fresh spray dried dispersion (SDD) for carbamazepine and tolfenamic acid with polymers exhibiting a high melt depression. On the other hand, melting point depression was low for all polymers tested for tolbutamide and partial crystallization was observed in the fresh SDD.

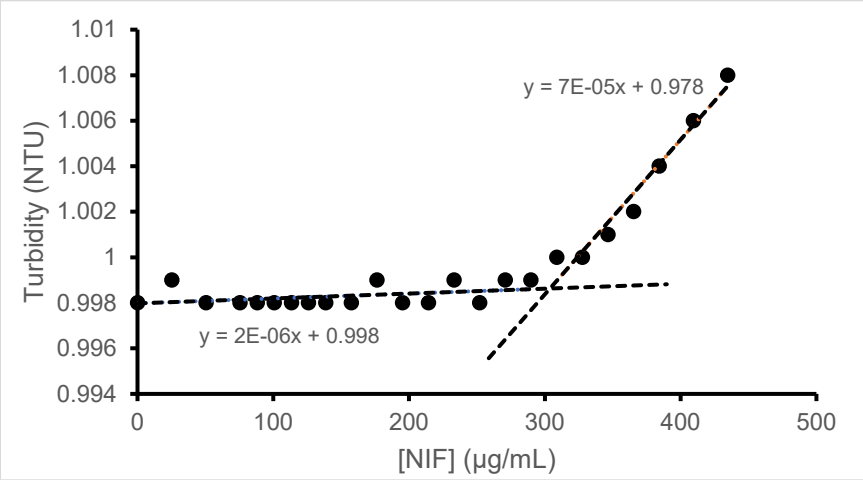

Figure 4. NIF amorphous solubility determination via turbidity method. Intersection of the two linear regressions indicate that the onset of turbidity increase correlated to the amorphous solubility.

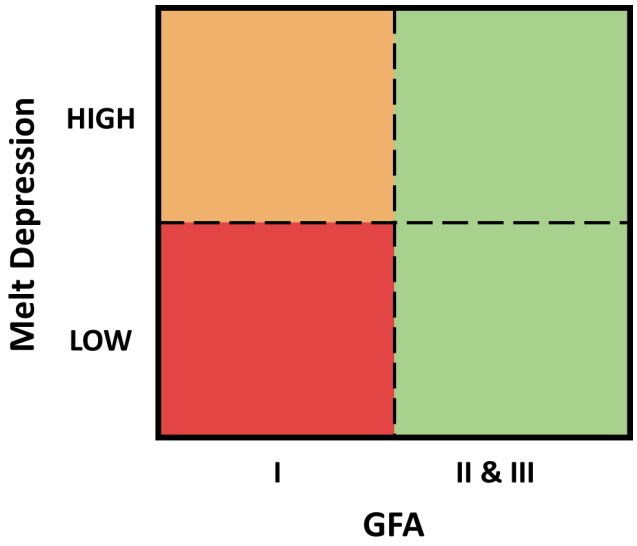

Figure 5. Proposed strategy for ASD development based on the drug-polymer melt depression and GFA class. Green indicates highly feasible, orange indicates possible, while red indicates unlikely for development.

Polymer Selection

Generally, the polymers screened for ASD are cellulose (HPMC, HPMCAS, HPMCP, or HPC), lactam (PVP, PVPVA, or Soluplus), or acrylic acid (PAA or Eudragit) based. These polymers are selected based on their T_g and miscibility. High T_g polymers, if miscible, will result in a single, high $T_{g,mix}$ of the resultant ASD. Fox and Gordon-Taylor equations are generally sufficient in predicting the resultant $T_{g,mix}$. $T_{g,mix}$ is also affected by the T_g of the drug, which is correlated to its melting point (T_m), i.e., the higher the T_m the higher the T_g of the drug. Therefore, based on $T_{g,mix}$ criteria alone, drugs with high T_m have a larger pool of polymers as candidates since polymers with lower T_g may still give a sufficiently high $T_{g,mix}$. While $T_{g,mix}$ indicates the strength of the resultant glass, miscibility evaluation is meant to indicate the homogeneity ("one-phaseness") of the drug-polymer mixture. It is widely accepted that intermolecular interaction, e.g., H-bond, between drug and polymer is thought to determine miscibility. Miscibility can be estimated via a solubility parameter, δ, calculation whereby little to no difference in solubility parameter between drug and polymer indicates favorable interaction. Marsac et al. [19] pioneered a unique approach for miscibility determination by combining melting point depression of drug-polymer physical mixture at varied drug loads and the Flory-Huggins theory, whereby a negative interaction parameter, χ, indicates favorable interaction and miscibility. While these techniques are commonly used, they are laborious and require accurate experimentation and calculation that is difficult to apply in the initial stage of polymer selection. Herein, the melting point depression approach with 1:1 (w/w) physical mixture of NIF-polymer was used to rapidly identify whether strong interaction exists between drug and polymer and rank order these polymers. Melting point depression with physical mixtures has been widely used especially in the drug-excipient compatibility field [20-22]. While generally an excipient displaying a strong interaction (evidenced by large melting point depression) tends to be undesirable in the drug-excipient field, this interaction is actually beneficial when developing an ASD (as long as no chemical degradation is observed). Among the

polymers screened (Figure 6), PVP and PVPVA exhibited the largest melting point depression and were selected as the lead polymers. While the NIF melt was only depressed by 4-8 °C with either PVP or PVPVA, the extent of melt depression is dependent on the heating rate used on the DSC (see Solid Solubility Determination section where larger melt depression was observed with a lower heating rate). Nevertheless, our internal studies with NIF and other model compounds (unpublished data) showed that lowering the heating rate did not affect those systems having minimal or no melt depression (it only accentuated systems that already show melt depression). Thus, the melt depression approach is sufficient to rapidly detect lead polymers for ASD development.

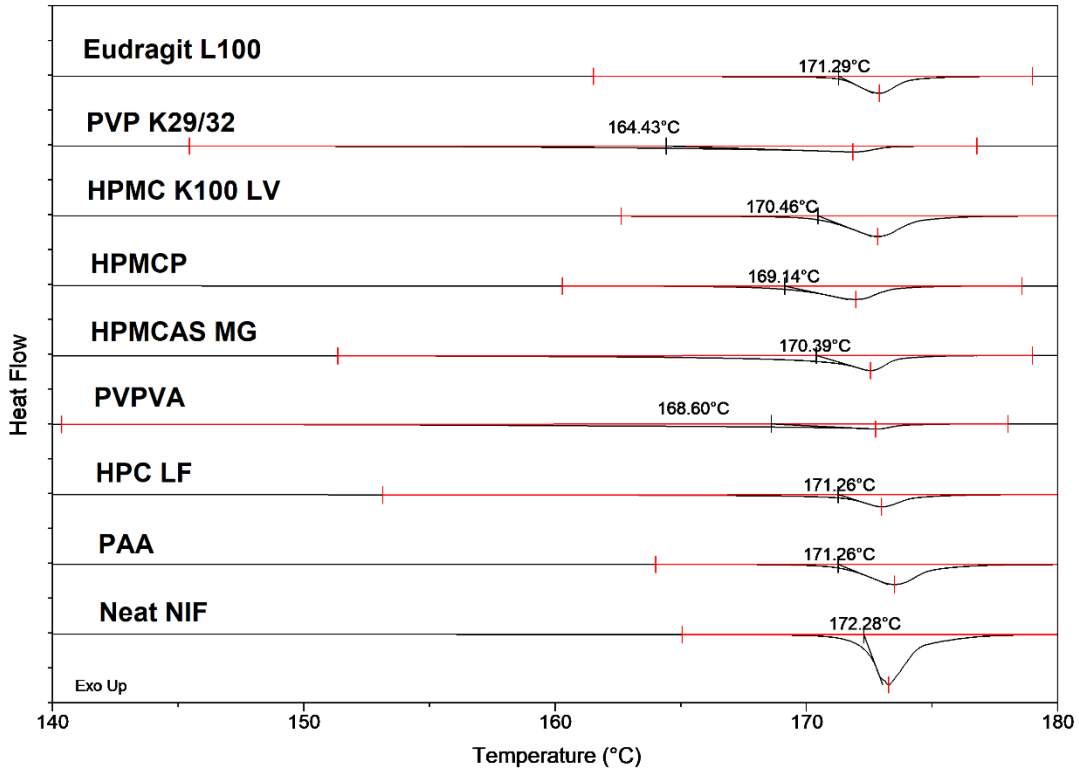

Figure 6. Melting point depression results of 1:1 (w/w) NIF-polymer physical mixture.

Solid Solubility Determination

Once lead polymers are selected, an approach to determine drug load in these polymers was developed by modifying the Kyerematenng approach [23]. This approach was used to determine crystalline drug solubility in the polymer. Figure 7 shows a general schematic of ASD phase behavior at various temperatures as a function of drug load. Two important parameters to be determined in this exercise are the T_g and solubility temperature (T_s). T_g values were determined by a cyclic mDSC method at a few drug loads and fitted for the remaining drug load by the Gordon-Taylor equation. T_s were

determined via the melt depression approach as described earlier (though with a slow heating rate of 1 °C/min) at a few drug loads and fitted for the remaining composition via a polynomial equation. Then, the solubility at room temperature can be extracted from the fitting. Once these important parameters are plotted, amorphous drug stability in the ASD can be clearly assessed. As discussed above, miscibility refers to the one-phaseness of a system. On the other hand, the solubility information provides the crystallization risk. Thus, while a miscible ASD is always desirable, there is a space where crystallization can be fully avoided. Ideally, one should develop an ASD in the subsaturated region to eliminate the risk of crystallization. However, this is not always possible as the drug solubility may be very low, which would cause a "pill burden" issue for patients. If solubility is low, one may develop an ASD in the supersaturated region as long as a miscible ASD can be generated followed by storage at $T=T_g$-50.

NIF phase behavior in PVP and PVPVA is shown in Figure 8. It is important to note that T_s at drug load <75% could not be determined for NIF-PVP system due to a plateau in the melting point (NIF melt remained constant below 75% drug load). This is likely due to the slow dissolution of NIF at temperatures near T_g of PVP, which is consistent with Kyerematenge's observation [23]. On the other hand, because PVPVA has a lower T_g than PVP, T_s can be determined at a much lower drug load in PVPVA. NIF room temperature solubility was found to be 34% and 2% for PVP and PVPVA, respectively. NIF solubility in PVPVA was found to be 3% in Kyerematenge's work, which confirmed our results. These values were then used as the initial drug load tested for both polymers.

A literature survey and our internal data suggest that drug solubility in polymer is low when melt depression at 1:1 w/w mixture (at a heating rate of 1 °C/min) is low. Low solubility here refers to solubility below 10% drug load which, if used as ASD drug load, will present a pill burden in the final drug product weight that may be impractical for patients to ingest. It is our observation that in order to achieve a meaningful solubility (≥10% drug load) a melt depression of ≥10 °C at 1:1 drug/polymer has to be demonstrated. In addition, our survey indicates that drug solubility as high as 30-40% can be achieved, although polymers that provide the highest solubility tend to be mostly lactam-based polymers, i.e., PVP, PVPVA, and Soluplus. Interestingly, this is consistent with the very strong H-bond accepting nature of the lactam (pyrrolidone) group [25], which is not present in other polymers. Furthermore, for high solubility to be observed, the drug must contain a strong H-bond donor or, in the case of NIF, a Brønsted acid N-H group. Indeed, a shift of ~60 cm^{-1} in the vibrational frequency of the N-H group of NIF has been observed previously in the freeze-dried formulation of NIF/PVP due to its strong interaction with the C=O group of PVP [26].

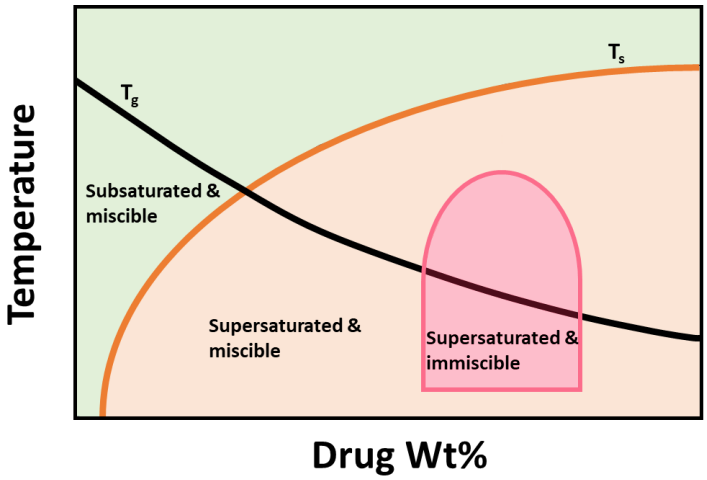

Figure 7. Modified temperature vs. composition graph from Prudic et al. [24]. T_g is represented in black line while solubility temperature (T_s) is the orange line. The area in green indicates a thermodynamically stable and miscible mixture. The orange area indicates a supersaturated and miscible system. The red area indicates a supersaturated and immiscible system.

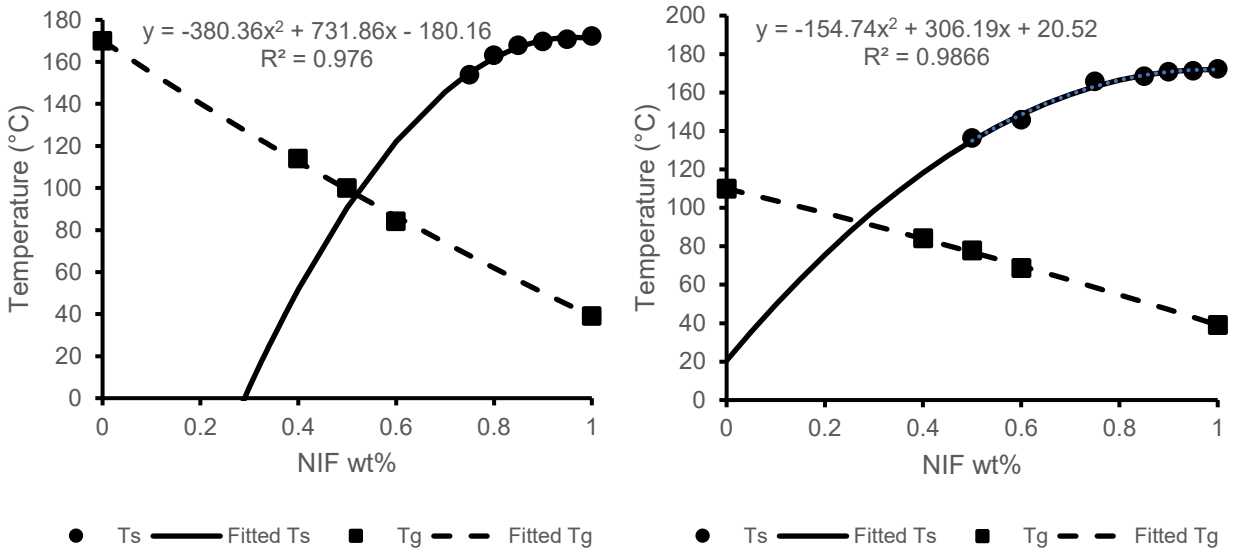

Figure 8. Solubility temperature (T_s) and $T_{g,mix}$ as a function of NIF wt%. NIF-PVP (left) and NIF-PVPVA (right) systems.

Characterization of NIF SDD

Once NIF solubility in our lead polymers was determined, NIF/polymer was spray dried at two different ratios (drug load): one at solubility and one above solubility. For PVP, 33% and 60% drug loads were chosen, while 4% and 50% were chosen for PVPVA. The PXRD patterns and mDSC thermograms of the initial spray dried dispersions (SDD) are shown in Figure 9 and Figure 10, respectively. No peaks were observed in all of the PXRD patterns suggesting X-ray amorphous phase for all of the SDD. However, while a single T_g was observed in most of the SDD which suggests a miscible system, several T_g's were observed for the 60:40 NIF/PVP suggesting that this dispersion was both supersaturated and immiscible or phase separated (red area in Figure 7). In addition, no birefringence was observed in all of the initial SDD created as evaluated by PLM (data not shown).

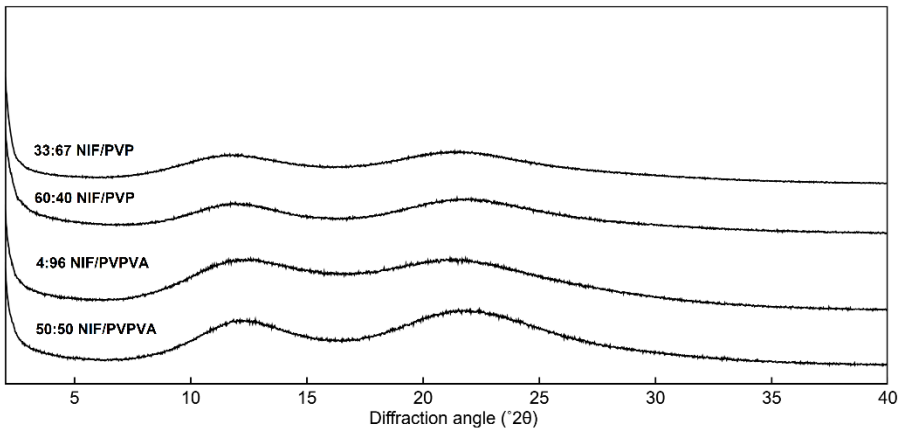

Figure 9. PXRD patterns of the initial NIF SDD.

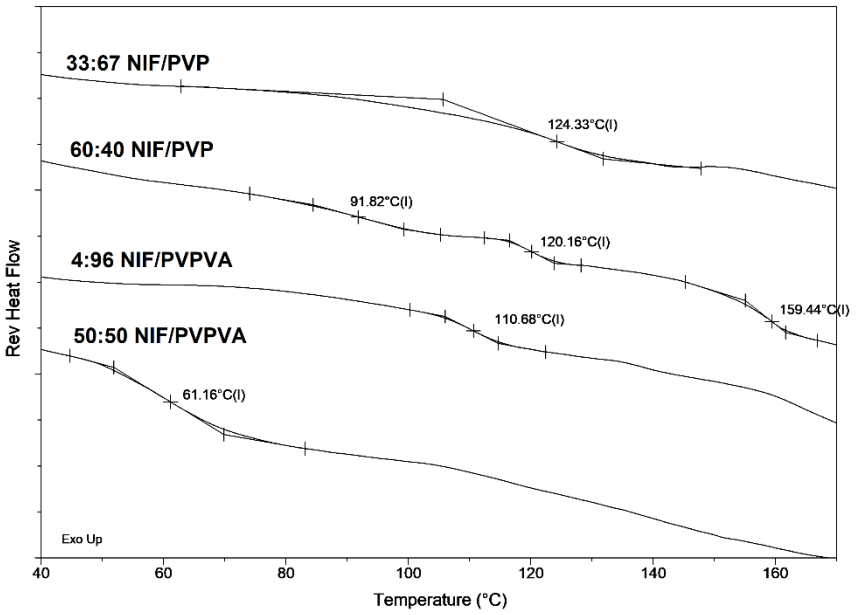

Figure 10. mDSC thermogram of the initial NIF SDD.

Stability Evaluation

It has been proposed that ASD prepared below the solubility (i.e., crystalline drug solubility in polymer) limit can be stored without regards to the T_g-50 rule, while those above the solubility limit must adhere to the rule for crystallization to be avoided. Herein, the four SDD were each stressed at $T_{storage}<T_g$-50 and $T_g>T_{storage}>T_g$-50. The results (Table 2) indeed confirm that for supersaturated ASD, the T_g-50 rule must be obeyed to maintain the amorphous phase. In addition, this rule was not critical for those below the solubility limit as demonstrated by the absence of crystallization even at elevated temperature of 100 °C. Unfortunately, the samples exposed at the higher temperatures showed discoloration after 3 weeks, suggesting chemical degradation; thus, the high temperature studies were discontinued. mDSC results were aberrant as the baseline was not consistent and determination of thermal events was challenging for most of these samples, except those samples below the solubility limit (33:67 NIF/PVP and 4:96 NIF/PVPVA) where no phase separation or crystallization was observed. Thus, PLM was used to evaluate crystallization in these samples via birefringence/extinction observation. PXRD was not used due to limited sample amount used in the stability studies.

Table 2. Stability of SDD following 3-weeks exposure to dry and varied storage temperatures.

SDD	Crystallized @ $T_{storage}<T_g$-50?	Crystallized @ $T_g>T_{storage}>T_g$-50?
33:67 NIF/PVP	No[1]	No[1]
60:40 NIF/PVP	No[2]	Yes[2]
4:96 NIF/PVPVA	No[1]	No[1]
50:50 NIF/PVPVA	No[2]	Yes[2]

[1]Stored at 40 and 100 °C for $T_{storage}<T_g$-50 and $T_g>T_{storage}>T_g$-50, respectively.
[2]Stored at 25 and 60 °C for $T_{storage}<T_g$-50 and $T_g>T_{storage}>T_g$-50, respectively.

Separately, the four SDD were also subjected to temperature/relative humidity (T/RH) conditions of 25 °C/60% RH and 40 °C/75% RH. The non-reversible (Figure 11) and reversible (Figure 12) heat flow showed that after 6 days of exposure to these conditions crystallization was only observed in systems at high drug load (solubility previously calculated no longer applies in these systems after moisture introduction) as evidenced by endotherm(s) above 145 °C, albeit 50:50 NIF/PVPVA system did not crystallize at 25 °C/60% RH. However, phase separation was observed in all of these systems as evidenced by the appearance of NIF T_g near 47 °C (see neat NIF T_g in Figure 3). In most of these systems, the T_g of polymer or remaining miscible ASD was difficult to detect. The water content in these systems after storage was 10-11 wt% and 4-6 wt% for the low and high drug load, respectively. No significant difference in water content was observed between 25 °C/60% RH and 40 °C/75% RH in these systems. The higher water content in low drug load is consistent with the fact that the polymer is much more hydrophilic and hygroscopic than NIF. The extent of moisture uptake by these SDD is consistent with those reported by Patel et al. [27]. Since phase separation was observed, this suggests that the solubility of NIF in PVP and PVPVA in the presence of moisture is now much lower than it was originally predicted for dry conditions (the boundaries of solubility line and immiscibility in Figure 7 have shifted to the left as a result of moisture in the samples). Thus, while high drug solubility can be achieved in lactam-based polymers, protection from moisture is critical due to the hygroscopic nature of these polymers.

Table 3. Stability of SDD following 6-days exposure of T/RH storage.

SDD	Crystallized @ 25 °C/60%RH?	Crystallized @ 40 °C/75%RH?
33:67 NIF/PVP	No	No
60:40 NIF/PVP	Yes	Yes
4:96 NIF/PVPVA	No	No
50:50 NIF/PVPVA	No	Yes

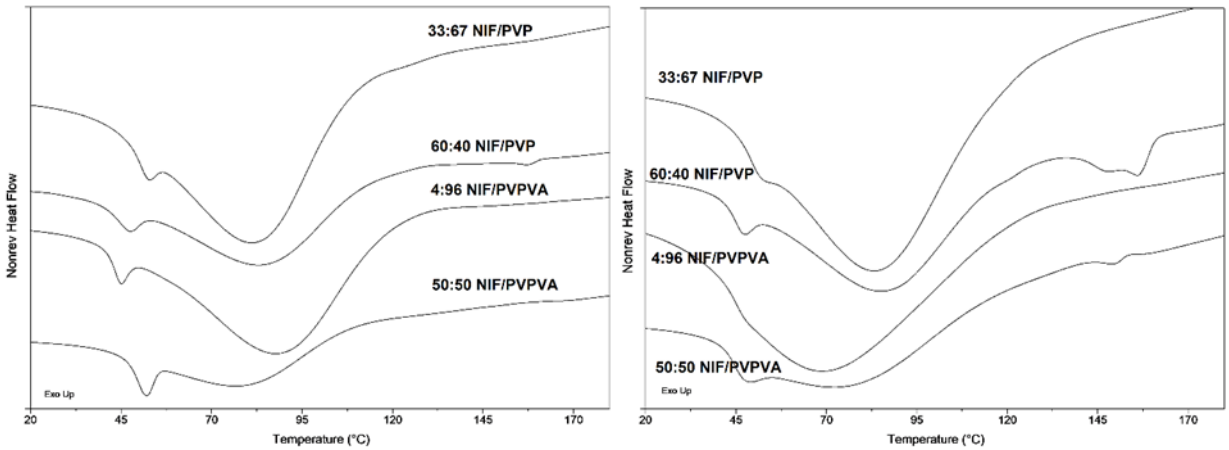

Figure 11. Non-reversible heat flow thermogram from SDD exposed to 25 °C/60% RH (left) and 40 °C/75% RH (right).

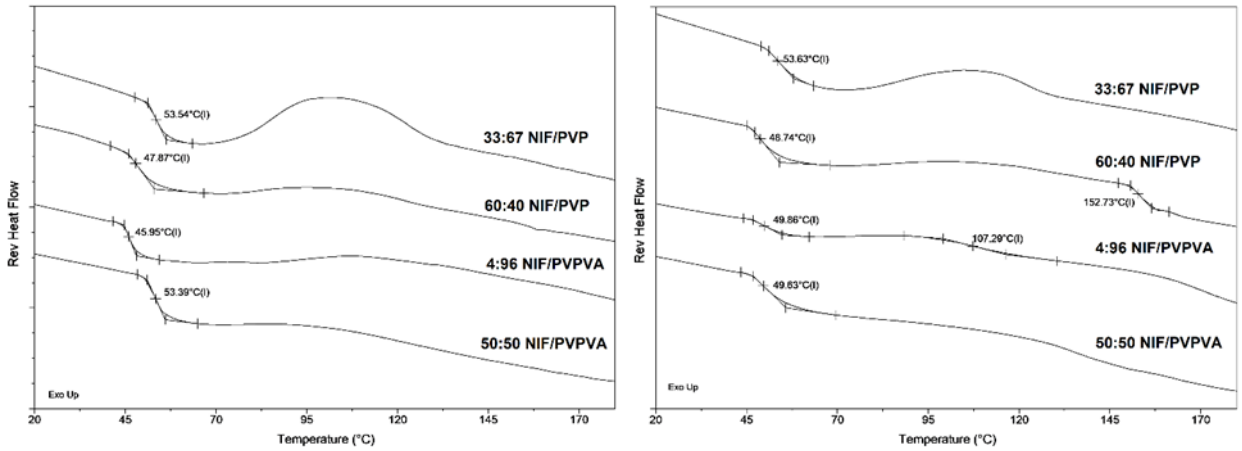

Figure 12. Reversible heat flow thermogram from SDD exposed to 25 °C/60% RH (left) and 40 °C/75% RH (right)

Performance Evaluation via *in vitro* Dissolution

While estimation of drug solubility in polymer is useful in predicting physical stability and storage recommendation, the drug load at solubility may not necessarily perform the best in *in vitro* dissolution (though it is possible that one could find a system with high solubility that rapidly dissolves). Herein, dissolution experiments were conducted with the crystalline NIF and NIF SDD generated above except the 4:96 NIF/PVPVA since a large amount would have to be added into the dissolution media. The results (Figure 13) showed a substantial improvement in dissolution rate and solubility of all SDD compared to crystalline NIF, as expected. Crystalline NIF did not reach its equilibrium solubility (see Initial Characterization) within 3 hours. However, while faster dissolution rates are observed in all the SDD evaluated, it is important to note that there appears to be a correlation between dissolution rate and drug load in the SDD. For instance, 33:67 NIF/PVP dissolved much more rapidly compared to 60:40 NIF/PVP SDD. A literature survey suggests that there is a limit of congruency in ASD dissolution whereby ASD dissolution is controlled by the surface component exposed to the aqueous media [28-30]. At low drug load, hydrophilic polymer dominates the surface of ASD, which in turn results in rapid, congruent drug/polymer dissolution. On the other hand, a hydrophobic drug dominates the surface of high drug load ASD, thus resulting in an incongruent drug/polymer dissolution with slow drug release. Furthermore, an ideal ASD should generate liquid-liquid phase separation (LLPS) upon introduction to aqueous media. When LLPS occurs, two liquid phases co-exist: aqueous solution containing dissolved drug and an oily drug-rich phase containing aggregated drug molecules.

It has been proposed that generation and maintenance of LLPS upon ASD dissolution would provide the maximum driving force for absorption as this is the highest achievable free drug concentration and rapid replenishment of free drug following intestinal permeation [12, 31]. In addition, the small-sized droplets of the second liquid (oily) phase would supplement the advantage of LLPS-generating ASD as they enable permeation through mucus layer in the lining of the intestinal wall [32-33]. The initial snapshot of our dissolution experiment (Figure 14) indeed showed that the rapidly-dissolving SDD of 33:67 NIF/PVP generated LLPS immediately upon aqueous contact, while the higher drug load with PVP or PVPVA showed poor wetting with solids floating on the media surface. Moreover, it was of interest to evaluate whether a change in polymer at 33% drug load, i.e., 33:67 NIF/PVPVA, would also result in a similar dissolution profile as 33:67 NIF/PVP. Figure 13 showed very similar dissolution profiles at 33% drug load between the two polymers and that a higher dissolution rate was achieved compared to 50:50 NIF/PVPVA. The results suggest that 33% NIF in either PVP or PVPVA can be selected as the lead ASD with a recommended storage of 25 °C/dry since this drug load is below the solubility limit for PVP system and much below the predicted $T_{g,mix}$ of ~90 °C for PVPVA system.

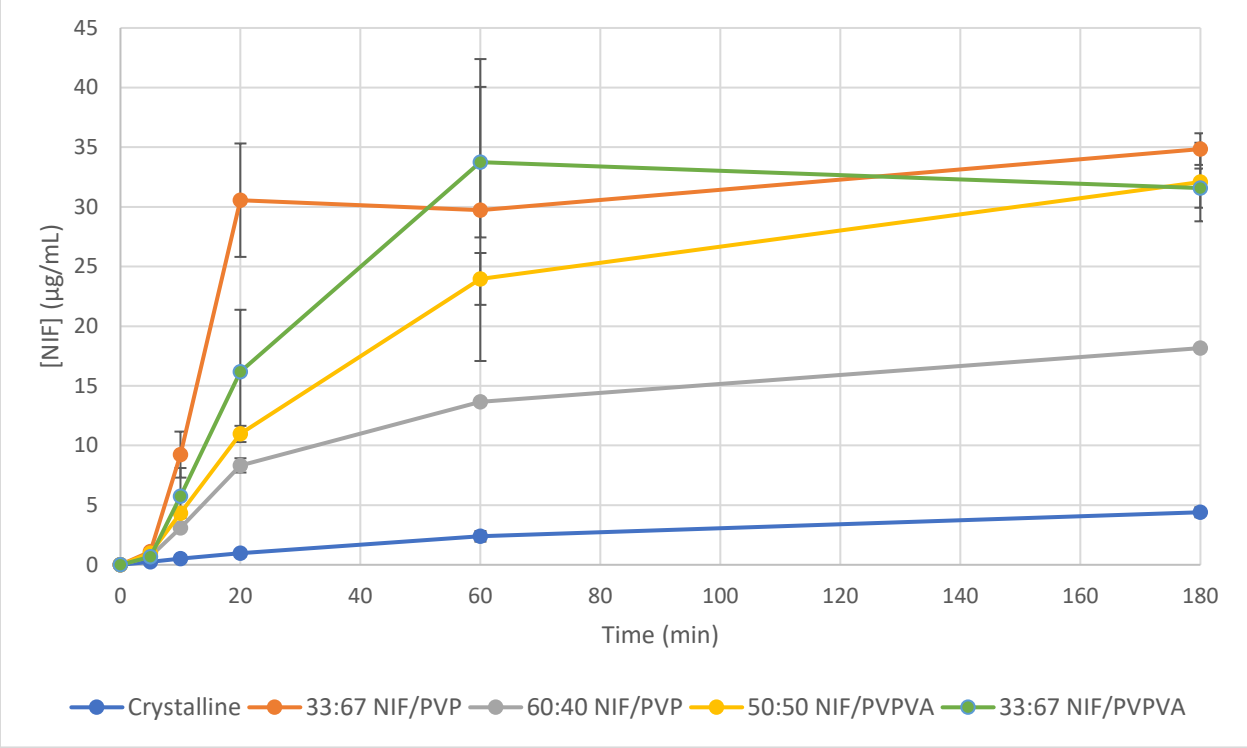

Figure 13. *In vitro* dissolution of crystalline NIF and NIF SDD in pH 6.8 buffer.

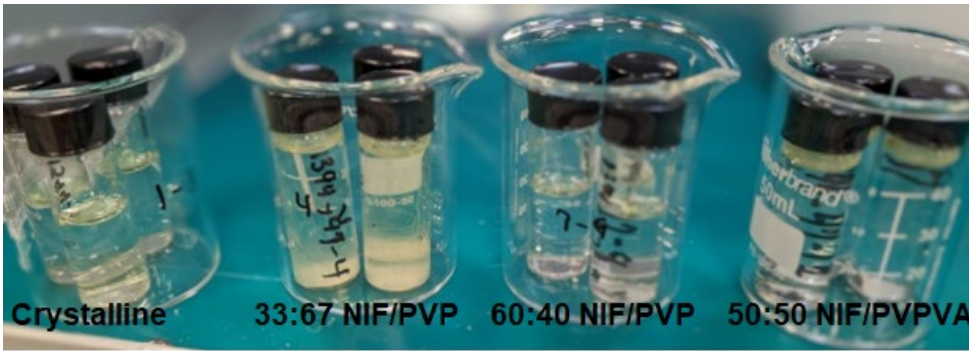

Figure 14. Initial snapshot of *in vitro* dissolution of crystalline NIF and NIF SDD.

The concentration at which LLPS was generated by SDD, i.e., 35 µg/mL, is much lower than the amorphous solubility determined in the Initial Characterization section. This discrepancy is likely due to the accumulation of NIF above the liquid surface during the amorphous solubility determination causing an overestimation. In addition, the presence of a high concentration of polymer in the SDD likely contributed to the change in the NIF amorphous solubility.

Development Timeline

The summary of steps used in the ASD development is shown in Figure 15. These steps, which involve very simple techniques and instrumentation, only take approximately two weeks from start to lead identification. While there are other factors, such as long-term stability and a scalable manufacturing process, that would take a considerable amount of time to establish, the steps presented herein will accelerate the initial feasibility and screening process.

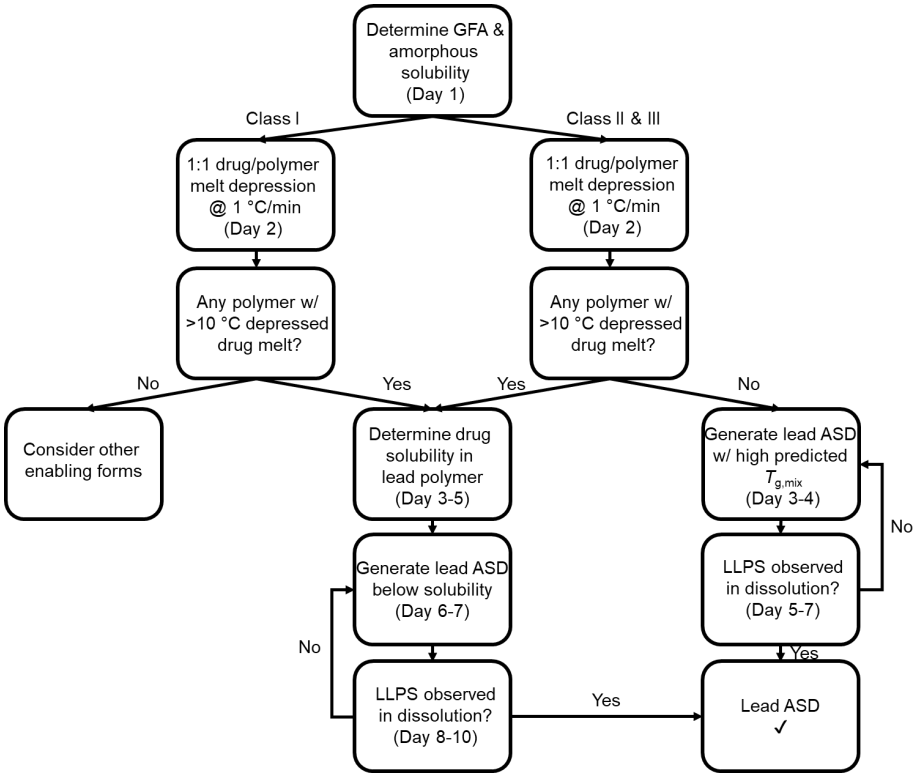

Figure 15. Proposed steps and timeline of ASD development.

Conclusion

An example of rapid development of ASD was presented by using collective advanced steps reported in the literature. Herein, NIF ASD were developed by selecting lead polymers with appropriate drug loads that provide sufficient physical stability and superior dissolution performance evidenced by LLPS generation. Surprisingly, the ASD development process only involved several simple experiments with a short timeline.

References

1. Patil, R., et al., *Optimized Hydrophobic Interactions and Hydrogen Bonding at the Target-Ligand Interface Leads the Pathways of Drug-Designing*, PLoS One, 5(8): e12029 (2010).
2. Tambe, S., et al., *Recent Advances in Amorphous Solid Dispersions: Preformulation, Formulation Strategies, Technological Advancements and Characterization*, Pharmaceutics 2022, 14(10), 2203.
3. Singhal, D., et al., *Drug polymorphism and dosage form design: a practical perspective*, Adv. Drug Del. Rev. 56 (2004) 335-347.
4. McNamara, D.P., et al., *Use of a Glutaric Acid Cocrystal to Improve Oral Bioavailability of a Low Solubility API*, Pharm. Res. 23, 1888-1897 (2006).
5. Schittny, A., et al., *Mechanisms of increased bioavailability through amorphous solid dispersions: a review*, Drug Del., 27:1, 110-127 (2020).
6. Carrier, R.L., et al., *The utility of cyclodextrins for enhancing oral bioavailability*, J. Cont. Rel., 123(2), 78-99 (2007).
7. Porter, C.J.H., et al., *Enhancing intestinal drug solubilisation using lipid-based delivery systems*, Adv. Drug Del. Rev., 60(6), 673-691 (2008).
8. Bhujbal, S.V., et al., *Pharmaceutical amorphous solid dispersion: A review of manufacturing strategies*, Acta Pharm. Sin. B 2021, 11, 2505-2536.
9. Baird, J.A., et al., *A Classification System to Assess the Crystallization Tendency of Organic Molecules from Undercooled Melts*, J. Pharm. Sci., Vol. 99, 3787-3806 (2010).
10. Hancock, B.C and Parks, M., *What is the true solubility advantage for amorphous pharmaceuticals?*, Pharm. Res. 17 , 397-404 (2000).
11. Murdande, S.B., et al., *Solubility advantage of amorphous pharmaceuticals: I. A thermodynamic analysis*, J. Pharm. Sci., Vol. 99(3), 1254-1264 (2010).
12. Ilevbare, G.A and Taylor, L.S., *Liquid-Liquid Phase Separation in Highly Supersaturated Aqueous Solutions of Poorly Water-Soluble Drugs: Implications for Solubility Enhancing Formulations*, Cryst. Growth Des. 2013, 13, 1497-1509.
13. Konno, H., et al., *Effect of polymer type on the dissolution profile of amorphous solid dispersions containing felodipine*, Eur. J. Pharm. Biopharm. 70(2), 493-499 (2008).
14. Qian, F., et al., *Drug–polymer solubility and miscibility: stability consideration and practical challenges in amorphous solid dispersion development*, J. Pharm. Sci. 99(7), 2941-2947 (2010).
15. Wegiel, L.A., et al., *Crystallization of Amorphous Solid Dispersions of Resveratrol during Preparation and Storage—Impact of Different Polymers*, J. Pharm. Sci. 102(1), 171-184 (2013).
16. Caira, M.R, et al., *Structural Characterization, Physicochemical Properties, and Thermal Stability of Three Crystal Forms of Nifedipine*, J. Pharm. Sci., Vol. 92, 2519-2533 (2003).
17. Gunn, E., et al., *Polymorphism of Nifedipine: Crystal Structure and Reversible Transition of the Metastable β Polymorph*, Cryst. Growth Des. 2012, 12, 2037-2043.
18. Zhang, W., et al., *Evaluation of accuracy of amorphous solubility advantage calculation by comparison with experimental solubility measurement in buffer and bio-relevant media*, Mol. Pharm, 2018, 15, 4, 1714-1723.
19. Marsac, P.J., et al., *Theoretical and Practical Approaches for Prediction of Drug-Polymer Miscibility and Solubility*, Pharm. Res., Vol. 23, No. 10, 2006.

20. Chadha, R. and Bhandari, S., *Drug-excipient compatibility screening – Role of thermoanalytical and spectroscopic techniques*, J. Phar. Biomed. Anal., 2014, 87, 82-97.
21. Narang, A.S., et al., *Excipient Compatibility*, Chapter 6 in Developing Solid Oral Dosage Forms: Pharmaceutical Theory and Practice, 2009.
22. Dave, V.S., et al., *Drug-Excipient Compatibility Studies in Formulation Development: Current Trends and Techniques*, AAPS FDD Section Newsletter, 2015, 9-15.
23. Kyerematen, S.O., et al., *A Fast and Reliable Empirical Approach for Estimating Solubility of Crystalline Drugs in Polymers for Hot Melt Extrusion Formulations*, J. Pharm. Sci., 103:2847-2858, 2014.
24. Prudic, A., et al., *Thermodynamic Phase Behavior of API/Polymer Solid Dispersions*, Mol. Pharm., 2014, 11(7):2294-304.
25. Eerdenbrugh, B.V. and Taylor, L.S., *An ab initio polymer selection methodology to prevent crystallization in amorphous solid dispersions by application of crystal engineering principles*, Cryst. Eng. Comm., 2011, 13, 6171.
26. Alqurshi, A., et al., *In-situ freeze-drying - forming amorphous solids directly within capsules: An investigation of dissolution enhancement for a poorly soluble drug*, Scientific Reports, 2017, 7.
27. Patel, N.G., Serajuddin, A.T.M, *Moisture sorption by polymeric excipients commonly used in amorphous solid dispersion and its effect on glass transition temperature: I. Polyvinylpyrrolidone and related copolymers*, Int. J. Pharm., Vol. 606, 2022, 121532.
28. Indulkar, A.S, et al., *Insights into the Dissolution Mechanism of Ritonavir–Copovidone Amorphous Solid Dispersions: Importance of Congruent Release for Enhanced Performance*, Mol. Pharm, 2019, 16, 3, 1327-1339.
29. Chailu, Q., et al., *Insights into the Dissolution Behavior of Ledipasvir–Copovidone Amorphous Solid Dispersions: Role of Drug Loading and Intermolecular Interactions*, Mol. Pharm, 2019, 16, 12, 5054-5067.
30. Deac, A., et al., *Dissolution Mechanisms of Amorphous Solid Dispersions: Role of Drug Load and Molecular Interactions*, Mol. Pharm, 2023, 20, 1, 722-737.
31. Indulkar, A.S., et al., *Exploiting the Phenomenon of Liquid–Liquid Phase Separation for Enhanced and Sustained Membrane Transport of a Poorly Water-Soluble Drug*, Mol. Pharm, 2016, 13, 6, 2059-2069.
32. Taylor, L.S. and Zhang, G.G.Z., *Physical chemistry of supersaturated solutions and implications for oral absorption*, Adv. Drug Delivery Rev., Vol. 101, 2016, 122-142.
33. Zhao, P., et al., *Liquid–liquid phase separation drug aggregate: Merit for oral delivery of amorphous solid dispersions*, J. Cont. Release, Vol. 353, 2023, 42-50.

Contact Information :

Triclinic Labs, Inc.
2660 Schuyler Ave., Suite A
Lafayette IN 47905
USA
TriclinicLabs.com
rfi@triclinicabs.com